REGULAR ARTICLE

blood advances

Mutations in the zebrafish *hmgcs1* gene reveal a novel function for isoprenoids during red blood cell development

Jose A. Hernandez,* Victoria L. Castro,* Nayeli Reyes-Nava, Laura P. Montes, and Anita M. Quintana

Department of Biological Sciences and Border Biomedical Research Center, University of Texas at El Paso, El Paso, TX

Key Points

- The products of the cholesterol synthesis pathway regulate RBC development during primitive erythropoiesis.
- Isoprenoids regulate erythropoiesis by modulating the expression of the GATA1 transcription factor.

Erythropoiesis is the process by which new red blood cells (RBCs) are formed and defects in this process can lead to anemia or thalassemia. The GATA1 transcription factor is an established mediator of RBC development. However, the upstream mechanisms that regulate the expression of *GATA1* are not completely characterized. Cholesterol is 1 potential upstream mediator of *GATA1* expression because previously published studies suggest that defects in cholesterol synthesis disrupt RBC differentiation. Here we characterize RBC development in a zebrafish harboring a single missense mutation in the *hmgcs1* gene (Vu57 allele). *hmgcs1* encodes the first enzyme in the cholesterol synthesis pathway and mutation of *hmgcs1* inhibits cholesterol synthesis. We analyzed the number of RBCs in *hmgcs1* mutants and their wild-type siblings. Mutation of *hmgcs1* resulted in a decrease in the number of mature RBCs, which coincides with reduced *gata1a* expression. We combined these experiments with pharmacological inhibition and confirmed that cholesterol and isoprenoid synthesis are essential for RBC differentiation, but that *gata1*a expression is isoprenoid dependent. Collectively, our results reveal 2 novel upstream regulators of RBC development and suggest that appropriate cholesterol homeostasis is critical for primitive erythropoiesis.

Introduction

Erythropoiesis is the process of producing and replenishing the number of circulating red blood cells (RBCs). There are 2 unique waves of erythropoiesis: the primitive and the definitive. Erythropoiesis is tightly controlled and regulated by a balance of cell proliferation, differentiation, and survival.[1,2] The overproduction of RBCs or lack of RBCs can cause human disease. Diamond-Blackfan anemia and sickle cell anemia are 2 examples of rare congenital anomalies that arise from defects in the production of RBCs,[3] and polycythemia occurs as a consequence of too many RBCs.[4-6] Genetic disorders of RBCs have revealed critical mediators of erythropoiesis,[7-11] many of which include transcription factors. For example, Diamond-Blackfan anemia can result from mutations in the transcription factor *GATA1*.[12-14] GATA1 is the founding member of the GATA family of zinc finger transcription factors[15] that interacts with a multitude of other proteins such as Friend of GATA, EKLF, SP1, p300, and PU.1 to promote erythropoiesis.[16]

Cholesterol is 1 known regulator of RBC function because it maintains the structure and integrity of the RBC membrane and aids in the protection against oxidative stress.[17-22] But both in vitro and in vivo studies have raised the possibility that cholesterol biosynthesis regulates the differentiation of RBCs.[23,24] Knockdown of *OSC/LSS*, which catalyzes the cyclization of monoepoxysqualene to lanosterol, decreased the self-renewing capacity of K562 cells in vitro and caused increased cell death of progenitor like cells. Follow-up in vivo assays have reinforced this premise as reduced cholesterol synthesis was associated with deficits in terminal RBC development.[24] These data provide strong evidence that cholesterol's function in RBCs is not restricted to membrane fluidity.

Submitted 9 August 2018; accepted 9 March 2019. DOI 10.1182/bloodadvances.2018024539.

*J.A.H. and V.L.C. contributed equally to this work.

For access to datasets and protocols, please contact the corresponding author by e-mail.

The full-text version of this article contains a data supplement.

The cholesterol synthesis pathway (CSP) begins with synthesis of HMG-CoA from aceto-acetyl-CoA, which then undergoes several transformations to produce farnesyl pyrophosphate. Farnesyl pyrophosphate represents a branch point in the pathway, ultimately resulting in the production of cholesterol or isoprenoids.[25-27] Both classes of lipids have diverse functions spanning membrane fluidity, protein prenylation, and precursors to various different types of molecules including vitamin D3. Cholesterol homeostasis has been previously linked to hematopoietic stem cell (HSC) differentiation,[28,29] and we confirmed that cholesterol synthesis is essential for RBC development.[24] The function of isoprenoids is less clear because isoprenoids give rise to diverse molecules, which themselves are critical for cell differentiation.[30-33]

Here we show that the products of the CSP are essential for RBC development. We show that defects in cholesterol and/or isoprenoids results in deficient numbers of RBCs, but that each lipid regulates RBC development by unique mechanisms. We show that inhibition of isoprenoid synthesis disrupts the number of Gata1$^+$ cells produced, but the inhibition of cholesterol has no effect on *gata1* expression or the number of Gata1$^+$ cells. Thus, we demonstrate an essential function for the CSP during RBC specification and primitive erythropoiesis.

Methods

Zebrafish care

For all experiments, embryos were obtained by crossing AB wild-type, Tupfel Long Fin wild-type, *Tg*(*gata1a*:dsRed)[34] or *hmgcs1*^{Vu57}.[35] All embryos were maintained in embryo medium at 28°C and all experiments were performed according to protocol 811689-5 approved by The University of Texas El Paso Institutional Animal Care and Use Committee. Genotyping was performed as previously described.[36]

Drug treatments and morpholino injection

Atorvastatin (pharmaceutical grade; Sigma, St. Louis, MO), lonafarnib (Sigma), and Ro 48 8071 (Santa Cruz Biotechnology, Santa Cruz, CA) were each dissolved in 100% dimethyl sulfoxide (DMSO). Treatment was initiated at the sphere developmental stage (~4-5 hours postfertilization [hpf]) and fresh drug was added every 18 to 24 hours until the harvest time points indicated in the figure legends. Drug concentrations were determined using a gradient of each drug (supplemental Figure 1) and the concentration selected was based on working conditions from previous literature. We selected a maximum tolerated sublethal dose producing a consistent phenotype according to a Fisher's exact test as previously described in Quintana et al.[36] Drugs were diluted in DMSO to make working solutions at the following concentrations: 2.0 μM atorvastatin,[35-37] 8 μM lonafarnib,[35,38] and 1.5 μM Ro 48 8071. Final concentration of DMSO was <0.01% in all samples and vehicle control treatment. Ro 48 8071 specificity for oxido-squalene synthesis has been previously described.[24,39,40] The specificity of lonafarnib has been previously described as a farnesyl protein transferase inhibitor.[41] For morpholino injections, antisense *hmgcs1* morpholinos (AATCATATAACGGTGTTGGTTCGTG) were injected (0.025 mM) at the single-cell stage and fixed at the indicated time points within the figure legend. For all treatment groups (drug treatment and morpholino) statistical significance was obtained using a Fisher's exact test.

o-dianisidine staining

o-dianisidine (Sigma) staining was performed as previously described by Paffett-Lugassy and Zon.[42] Briefly, embryos were harvested at the desired time point and stained in the dark for 15 minutes at room temperature with *o*-dianisidine (Alfa Aesar, Ward Hill, MA) (0.6 mg/mL), 0.01 M sodium acetate (Fisher, Waltham, MA), 0.65% H_2O_2 (Fisher), and 40% ethanol (Fisher). Stained embryos were fixed with 4% paraformaldehyde (Electron Microscopy Sciences, Hatfield, PA) for 1 hour at room temperature and bleached using 3% H_2O_2 and 2% potassium hydroxide (Fisher) for 12 minutes. Embryos were washed with phosphate buffered saline (PBS) and stored in 4°C. Embryos were imaged with Zeiss Discovery Stereo Microscope fitted with Zen Software.

Hemoglobin quantification

For hemoglobin quantification, larvae (numbers indicated in each figure) were homogenized with a pestle in purified water at 4 days postfertilization (dpf). Hemoglobin was measured with the Hemoglobin Assay Kit (Sigma-Aldrich) according to manufacturer's protocol. For analysis of the Vu57 allele, larvae were separated via distinct phenotypic hallmarks described previously.[35,36] The control contained both homozygous wild-type and heterozygous individuals harboring the Vu57 allele. Experiments were performed in a minimum of biological duplicate. For drug treatment assays, wild-type embryos were treated as described before assaying for hemoglobin concentration. Statistical significance was determined using a Student *t* test.

Whole mount in situ hybridization and quantitative real-time polymerase chain reaction

Whole mount in situ hybridization was performed as described by Thisse and Thisse.[43] Briefly, embryos were harvested and dechorionated at the indicated time point and fixed in 4% paraformaldehyde (Electron Microscopy Sciences) for 1 hour at room temperature. Embryos were dehydrated using a methanol:PBS gradient and stored in 100% methanol overnight in −20°C. Embryos were rehydrated using PBS:methanol gradient, washed in PBS with 0.1% Tween 20, and permeabilized with proteinase K (10 μg/mL) for the time indicated by Thisse and Thisse.[43] Permeabilized embryos were prehybridized in hybridization buffer (HB) (50% deionized formamide (Fisher), 5X SSC (Fisher), 0.1% Tween 20 (Fisher), 50 μg/mL heparin (Sigma), 500 μg/mL of RNase-free tRNA (Sigma), 1M citric acid (Fisher) (460 μL for 50 mL of HB) for 2 to 4 hours and then incubated overnight in fresh HB with probe (*gata1a* 75 ng, *hbbe1.1* 75 ng, *alas2* 150 ng) at 70°C. Samples were washed according to protocol, blocked in 2% sheep serum (Sigma), 2 mg/mL bovine serum albumin (Sigma) for 2 to 4 hours at room temperature, and incubated with anti-DIG Fab fragments (1:10 000) (Sigma) overnight at 4°C. Samples were developed with BM purple AP substrate (Sigma) and images were collected with a Zeiss Discovery Stereo Microscope fitted with Zen Software. Statistical analysis was performed using a Fisher's exact test. For quantitative polymerase chain reaction (qPCR), RNA was isolated from embryos at the indicated time point using Trizol (Fisher) according to manufacturer's protocol. Reverse transcription was performed using iScript (Bio-Rad, Redmond, WA) and total RNA was normalized across all samples. PCR was performed in technical triplicates for each sample using an Applied Biosystem's StepOne Plus machine with Applied Biosystem's software. Sybr green (Fisher) based primer pairs for each gene analyzed are as

follows: *gata1a* fwd GTTTACGGCCCTTCTCCACA, *gata1a* rev CACATTCACGAGCCTCAGGT, *hbbe1.1* fwd TGAATCCAGCACCCATCTGA, *hbbe1.1* rev CTCCGAGAAGCTCCACGTAG, *rpl13a* fwd TCCCAGCTGCTCTCAAGATT, *rpl13a* rev TTCTTGGAATAGCGCAGCTT. Analysis performed using $2^{\Delta\Delta ct}$. Statistical analysis of messenger RNA (mRNA) expression was performed using a Student *t* test. All qPCR was performed in biological duplicate or triplicate.

Confocal imaging

Embryos were fixed at the given time point and then mounted in 0.6% low-melt agar in a glass bottom dish (Fisher). Imaging was performed on a Zeiss LSM 700 at 20× magnification. Images were restricted to the caudal hematopoietic tissue. For each fish, a minimum of 12 to 20 *z*-stacks were collected. Statistical significance was obtained using a Student *t* test.

Results

Mutations in *hmgcs1* disrupt RBC development

Based on previous data,[24] we sought to determine the number of mature RBCs in a zebrafish harboring mutations in the *hmgcs1* gene (Vu57). The Vu57 allele introduces a single missense mutation (H189Q) in the *hmgcs1* gene, which encodes the first enzyme in the CSP. The Vu57 allele abrogates cholesterol synthesis, causing a multiple congenital anomaly syndrome characterized by defects in myelination, myelin gene expression, cardiac edema, pigment defects, and craniofacial abnormalities.[35,36] We first detected the number of hemoglobinized RBCs in Vu57 homozygous mutants (*hmgcs1* $^{-/-}$) or their wild-type siblings with *o*-dianisidine at 4 dpf. Over the first 4 days of development, all of the circulating RBCs are derived from primitive erythropoiesis; therefore, analysis of hemoglobinized RBCs at day 4 accurately depicts deficiencies in primitive erythropoiesis.[44] Wild-type siblings had adequate numbers of hemoglobinized RBCs throughout development and, at 4 dpf, the RBCs lined the ventral head vessels of the neck and face (Figure 1A). Homozygous carriers of the Vu57 allele had a reduced number of cells populating the ventral head vessels with some detectable circulating RBCs near the base of the yolk sac in a select number of individuals (Figure 1A-B).

We next quantified the decrease in circulating RBCs in homozygous mutants and their siblings. We performed a quantitative measure of total hemoglobin content using a colorimetric assay in which endogenous hemoglobin can be measured quantitatively at a wavelength of 400 nm.[45] To measure the levels of hemoglobin in siblings and Vu57 carriers, homozygous Vu57 larval were separated according phenotype at 3 dpf[35] and the total hemoglobin content of homozygous carriers was compared with the hemoglobin content of wild-type and heterozygous siblings at 96 hpf. Phenotypic hallmarks of the Vu57 allele include craniofacial abnormalities and cardiac edema.[35] As shown in Figure 1C, we detected a moderate, but consistent and statistically significant 20% decrease in total hemoglobin content ($P < .05$). Taken together, these data suggest that mutation of *hmgcs1* disrupts RBC development.

Mutation of *hmgcs1* disrupts the expression of markers associated with RBC differentiation

One possible explanation for the decrease in total hemoglobin content observed in larvae carrying the Vu57 allele could stem from an inability to produce globin mRNA. To determine whether mutations in *hmgcs1* interfere with globin expression, we performed whole mount in situ hybridization (ISH) at 26 hpf with an anti-*hbbe1.1* riboprobe. *hbbe1.1* was expressed in the caudal intermediate cell mass (ICM) of wild-type siblings and the onset of circulation was readily apparent as *hbbe1.1* mRNA was detected over the yolk sac (Figure 2A). *hbbe1.1* expression was upregulated in Vu57 embryos with expression that localized throughout the entire ICM and was not restricted to the most caudal region (Figure 2B, arrowhead). In addition, *hbbe1.1* expression over the yolk sac was increased relative to wild-type siblings at 26 hpf (Figure 2A-B).

We next measured the expression of *alas2*, which encodes the first enzyme in heme biosynthesis.[46] Wild-type siblings expressed appropriate *alas2* expression in the caudal ICM at 26 hpf (Figure 2C), but the level of *alas2* in embryos with the Vu57 allele was spatially disrupted spanning the entire ICM (Figure 2D, arrowhead) and increased relative to wild-type siblings. These data are consistent with the level and spatial expression of *hbbe1.1* because *alas2* is known to modulate the levels of globin.[47] We attempted to validate our collective expression analysis at 26 hpf by detecting hemoglobinized RBCs with *o*-dianisidine; however, we did not consistently or accurately detect hemoglobinized RBCs at 24-26 hpf ($n = 20$) in wild-type individuals (data not shown). These data are consistent with previous studies demonstrating that very few heme containing RBCs enter circulation before 30 hpf.[48,49] However, our mRNA expression analysis demonstrates that mutant embryos maintain the expression of globin and some of the enzymes necessary for heme synthesis.

gata1a expression is decreased in *hmgcs1* mutant embryos

Given the abnormal expression of globin (*hbbe1.1*), we hypothesized that the mutation of *hmgcs1* disrupts the expression of *GATA1*, a known regulator of globin expression. We measured the expression of *gata1a*, the zebrafish ortholog of *GATA1* using ISH and qPCR at 18 somites and 26 hpf in mutants and their wild-type siblings. At 18 somites, wild-type siblings expressed *gata1a* in the caudal ICM (Figure 3A, dorsal view), but the Vu57 allele resulted in decreased *gata1a* expression (Figure 3A-B, arrowheads). This decrease in *gata1a* persisted through the onset of circulation; we observed reduced *gata1a* expression at 26hpf (Figure 3C-D, arrowhead). We next quantified the expression of *gata1a* by qPCR. We quantified the expression of *gata1a* in embryos injected with an *hmgcs1* morpholino because genotyping of mutant larvae before RNA isolation could not be consistently achieved without rapid decay in total RNA quality. Microinjection of *hmgcs1* morpholinos accurately phenocopied the RBC deficits observed with the Vu57 allele (supplemental Figure 2) and QPCR confirmed a near 70% reduction in *gata1a* expression in morphants (Figure 3A-D,I, $P < .05$).

We next measured *gata1a* expression in wild-type embryos treated with 2 μM atorvastatin (ATOR), a drug that inhibits the rate-limiting step of the CSP,[50] and should mimic the effects of mutations in *hmgcs1*. *gata1a* expression was decreased in ATOR-treated embryos relative to vehicle control (Figure 3E-F, arrowheads; $P = .0001$) and qPCR confirmed that ATOR treatment caused a significant reduction in *gata1a* expression (Figure 3J, $P < .05$). We next confirmed these results by treating *Tg*(*gata1a*:dsRed) larvae with 2 μM ATOR or vehicle control. Treatment with ATOR caused ~50% decrease in the number of dsRed positive cells (Figure 3G-H,K, $P = 7.25273e\text{-}07$).

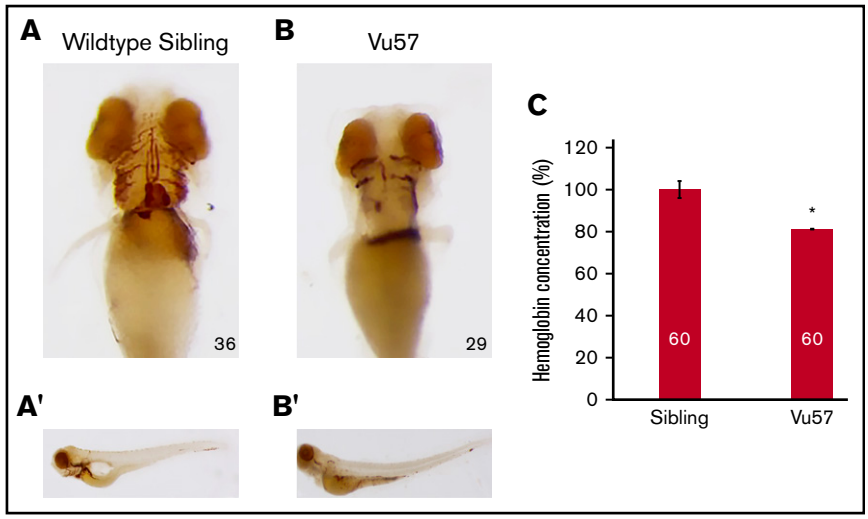

Figure 1. Mutations in *hmgcs1* cause a decrease in hemoglobinized RBCs. (A-B) *hmgcs1*$^{-/-}$ (Vu57) and their wild-type siblings (*hmgcs1*$^{+/+}$) were stained for hemoglobinized RBCs at 4 dpf (n = 36 *hmgcs1*$^{+/+}$, n = 29 *hmgcs1*$^{-/-}$) using *o*-dianisidine. Ventral views (A-B) of the hemoglobinized RBCs are shown with full body images (A′-B′) of both wild-type siblings and homozygous mutants (Vu57). The phenotype was completely penetrant in homozygous mutants. Total numbers of animals were obtained across a minimum 3 biological replicates. Images were taken with a 10× optical lens at 8× (A-B) and 6.3× (A′-B′) objective zoom. (C) The concentration of hemoglobin was measured in siblings (a pool of wild-type and heterozygous individuals) and embryos carrying the Vu57 allele. The assay was performed with 2 biological replicates with a total of 60 larvae. *$P < .05$.

Collectively, these data suggest that the Vu57 allele results in decreased numbers of Gata1a^{+} cells during primitive erythropoiesis.

Cholesterol and isoprenoids regulate RBC development

Mutation of *hmgcs1* disrupts the first enzyme of the CSP,[35] effectively interfering with the production of both cholesterol and isoprenoids. Recent evidence suggests that each of these 2 lipids can regulate the same biological process, but by independent molecular and cellular mechanisms.[35,36,38] We hypothesized that the defects observed in mutant larvae are cholesterol dependent. We treated wild-type embryos with either vehicle control (DMSO), 1.5 μM Ro 48 8071, to inhibit cholesterol, but not isoprenoids, and 8 μM lonafarnib, to inhibit farnesylated isoprenoids, but not cholesterol or 2 μM ATOR, a control to mimic the Vu57 allele. According to *o*-dianisidine, vehicle-treated embryos (DMSO) exhibited the appropriate number and spatial organization of RBCs in the ventral head vessels at 4 dpf (Figure 4A). Notably, treatment with ATOR induced a cerebral hemorrhage that was not consistent with the Vu57 allele (Figure 4B). Embryos treated with 1.5 μM Ro 48 8071 or 8 μM lonafarnib had visibly fewer RBCs (Figure 4A-D, $P = .0001$), suggesting that cholesterol synthesis is required for RBC development. Cerebral hemorrhages were not observed on treatment with Ro 48 8071 or lonafarnib. We further quantified the total hemoglobin content from larvae treated with each drug or vehicle control. As shown in Figure 4E, treatment with each drug resulted in a statistically significant decrease in total hemoglobin content. Drug treatment resulted in a more marked decrease in hemoglobin concentration relative to larvae harboring the Vu57 allele (Figure 1). This can likely be attributed to the fact that we performed a comparison between homozygous carriers of the Vu57 allele with a pool of heterozygous and wild-type homozygous individuals, suggesting that heterozygous individuals demonstrate some degree of deficits in RBC development. Taken together, these data raise the possibility that the synthesis of cholesterol and isoprenoids is essential for RBC development/differentiation.

gata1a expression is isoprenoid dependent

The Vu57 allele results in decreased *gata1a* expression and increased *hbbe1.1* expression. Therefore, we measured the expression of each gene in wild-type embryos treated with vehicle control (DMSO), 1.5 μM Ro 48 8071, or 8 μM lonafarnib using ISH at 26 hpf. *hbbe1.1* expression was localized to the caudal most region of the ICM and over the yolk sac in vehicle control embryos (Figure 5A). Inhibition of

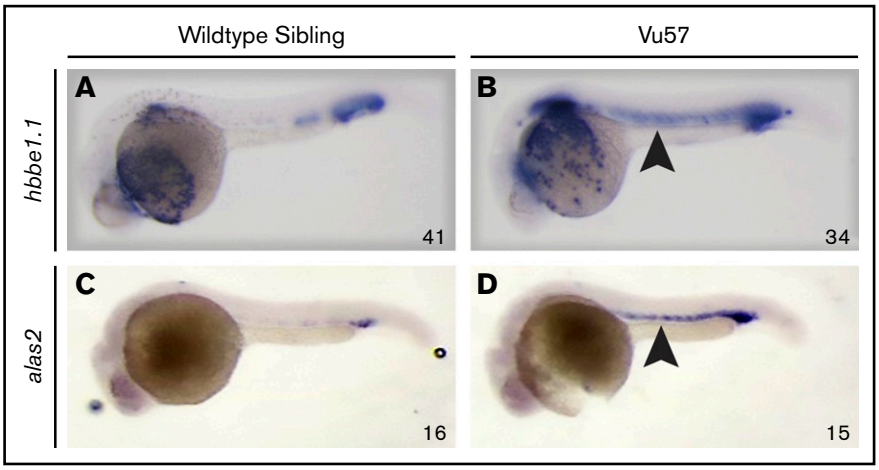

Figure 2. *hbbe1.1* and *alas2* are expressed in *hmgcs1* mutant larvae. Whole mount ISH was performed to detect the expression of *hbbe1.1* (n = 41 *hmgcs1*$^{+/+}$ [sibling], n = 34 *hmgcs1*$^{-/-}$ [Vu57]), (A-B) or *alas2* (n = 16 *hmgcs1*$^{+/+}$ [sibling], n = 15 *hmgcs1*$^{-/-}$ [Vu57]), (C-D) at 26 hpf. Purple, expression of each gene in the ICM; arrowhead, areas of increased or abnormal expression. Total number of animals was achieved with a minimum of 2 biological replicates. Images were taken with a 10× optical lens at 6.3× objective zoom.

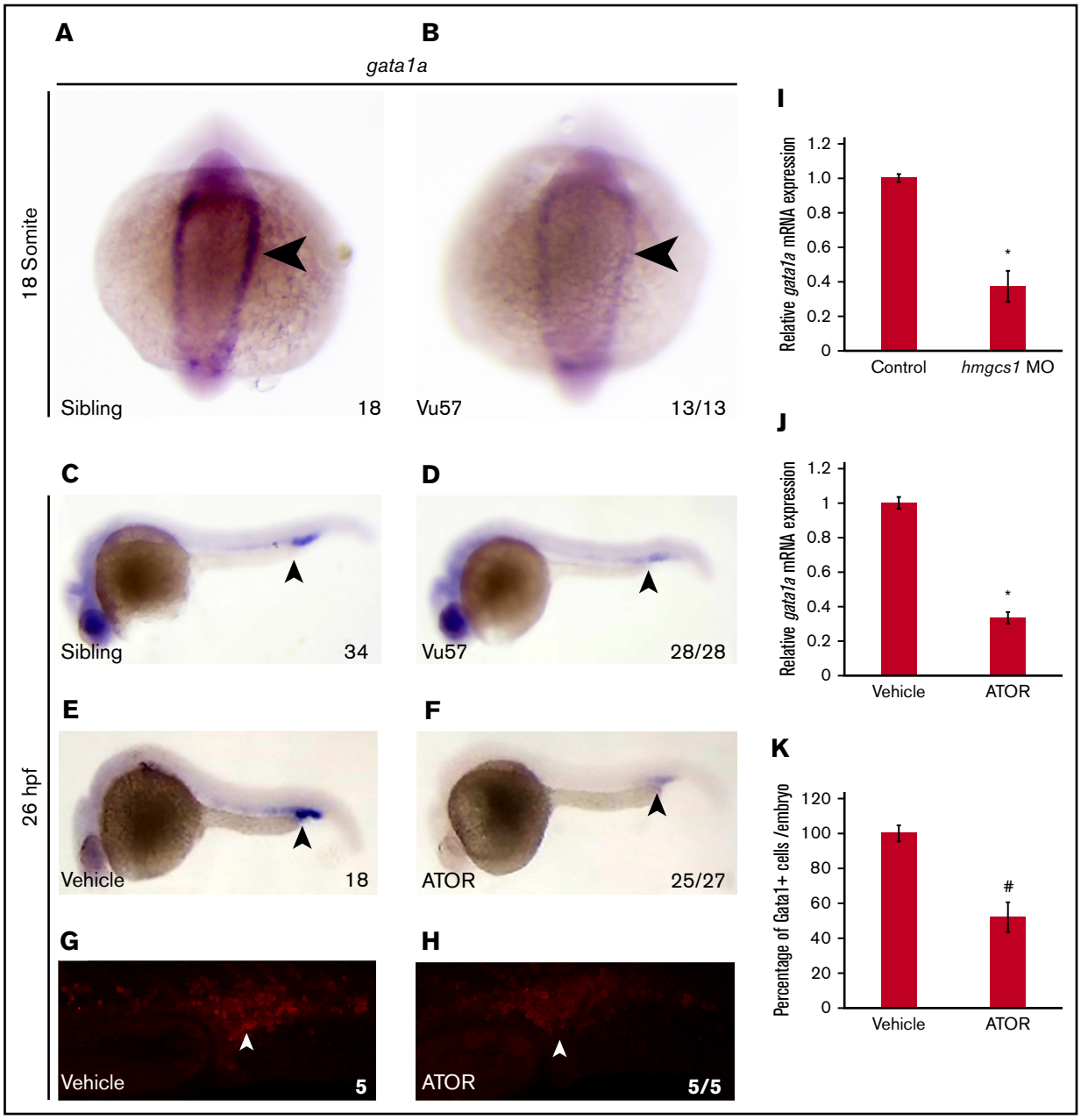

Figure 3. Mutation of *hmgcs1* disrupts *gata1a* expression. (A-D) Whole mount ISH was performed to detect the expression of the *gata1a* transcription factor at the 18-somite stage (n = 18 *hmgcs1*$^{+/+}$ [sibling], n = 13 *hmgcs1*$^{-/-}$ [Vu57]) and 26 hpf (n = 34 sibling, n = 28 Vu57). Total numbers of animals was obtained with a minimum of 2 biological replicates. (E-F) Embryos were treated with vehicle control (DMSO) or 2 μM ATOR (n = 18 DMSO, n = 27 ATOR, $P = .0001$) from sphere stage to 26 hpf and subjected to ISH to detect *gata1a* expression. Numbers of embryos affected are indicated below each figure. *P* value represents Fisher's exact test demonstrating the numbers affected per treatment group. Total numbers of embryos were obtained across 2 biological replicates. Arrowheads, area of *gata1a* expression at each time point. Images were taken with a 10× optical lens at 8× (A-B) and 6.3× (C-F) objective zoom. (G-H) *Tg*(*gata1a*:dsRed) embryos were treated with vehicle control (DMSO) or 2 μM atorvastatin. Fluorescence was visualized using a confocal microscope at 20× magnification. The number of cells/Z-stack was quantified using ImageJ. (I) Antisense *hmgcs1* morpholinos were injected (0.025 mM) at the single-cell stage and total RNA was extracted at the 18-somite stage. qPCR was performed to detect the expression of *gata1a*. All samples were performed in technical triplicate; error bars represent the standard deviation of technical triplicates. *$P < .05$. (J) Total RNA was isolated from embryos treated with vehicle control or ATOR and qPCR was performed to detect the expression of *gata1a*. All samples were performed in technical triplicate and error bars represent the standard deviation of technical triplicates. *$P < .05$. (K) Quantification of the number of dsRed cells from panels G and H. #$P = 7.25273e-07$.

cholesterol or isoprenoids caused a statistically significant increase in *hbbe1.1* mRNA (Figure 5G, $P < .05$) that was visible over the yolk sac (Figure 5A-C, $P = .0001$). The level and spatial expression of *hbbe1.1* is consistent with those observed in embryos carrying the Vu57 allele (Figure 2). Interestingly, the expression of *gata1a* was not affected by treatment with 1.5 μM Ro 48 8071, but

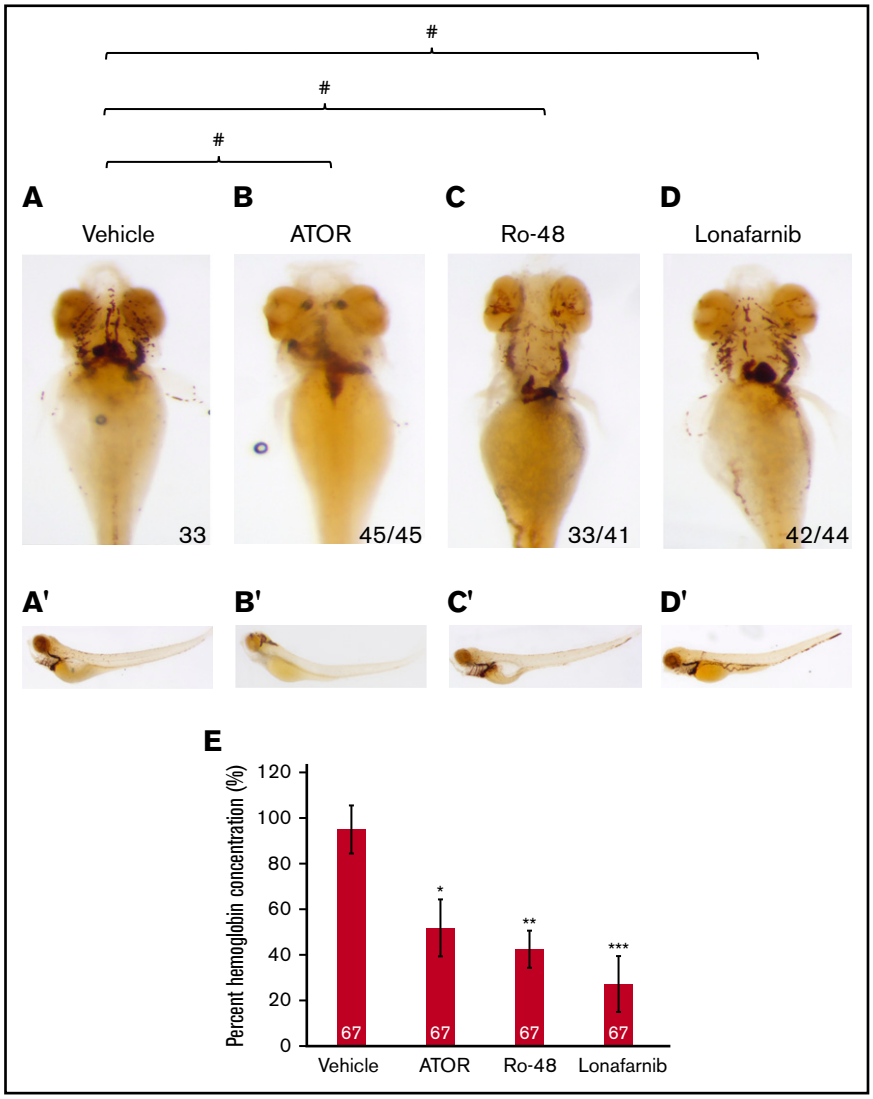

Figure 4. Cholesterol and isoprenoids regulate erythropoiesis. (A-D) Embryos were treated at sphere stage with ATOR, Ro 48 8071 (Ro-48) to inhibit cholesterol, lonafarnib to inhibit isoprenoids, or vehicle control (DMSO). At 4 dpf, embryos (n = 33 DMSO, n = 45 ATOR, n = 41 Ro-48, and n = 44 lonafarnib) were stained with *o*-dianisidine to observe mature RBCs. (A′-D′) Full body images of stained larvae at 4 dpf. Images were taken with a 10× optical lens at 8× (A-D) and 6.3× (A′-D′) objective zoom. $^{\#}P = .0001$. *P* value indicates the number of affected embryos affected is statistically significant according to Fisher's exact test. (E) The concentration of hemoglobin was measured in embryos treated with ATOR, Ro-48 to inhibit cholesterol, lonafarnib to inhibit isoprenoids, or vehicle control (DMSO) at 4 dpf. The number indicates total larvae analyzed across 3 biological replicates. $^{*}P = .000381218$, $^{**}P = 2.20098e\text{-}05$, $^{***}P = 1.42e\text{-}05$.

was significantly decreased when isoprenoid synthesis was inhibited (Figure 5D-F,H, $P < .05$). The decrease in *gata1a* expression was consistent with a decrease in the number of Gata1^{+} cells as demonstrated by the *Tg*(*gata1a*:dsRed) (Figure 5I, $P = 2.7125e\text{-}07$). Collectively, these data suggest that isoprenoids regulate RBC differentiation in a *gata1a* dependent manner.

Discussion

Here we show that cholesterol and isoprenoids regulate erythropoiesis using a zebrafish harboring mutations in the *hmgcs1* gene (Vu57 allele). Mutations in human *HMGCS1* have not been associated with disease, but there are 8 congenital anomalies that occur as a consequence of mutations within other enzymes of the CSP.[5-11,13,51] These congenital anomalies are characterized by diverse phenotypes,[7,21,51-53] and mutations in the zebrafish *hmgcs1* gene mimic these disorders, resulting in a multiple congenital anomaly syndrome. Therefore, zebrafish with mutations in *hmgcs1* have the potential to reveal novel cellular and molecular mechanisms underlying individual phenotypes across multiple genetic disorders.

Cholesterol represents approximately one-half the weight of an RBC membrane and governs membrane fluidity, transport, reversible deformations, and survival in response to oxidative stress.[54,55] In addition, cholesterol is a precursor for multiple molecules including bile acid, vitamin D, and steroid hormones. Moreover, deficiencies in cholesterol synthesis interfere with proper RBC development.[23,24] Based on these data, we hypothesized that mutation of *hmgcs1* would disrupt erythropoiesis in vivo. We found that homozygous mutation of *hmgcs1* causes a decrease in the number of hemoglobinized RBCs and total hemoglobin content, consistent with previous work,[24] demonstrating that defects in RBC number can be rescued by the exogenous injection of water-soluble cholesterol. Our study using the Vu57 allele establishes that the products of the CSP are essential for proper RBC homeostasis; however, the mechanisms by which the CSP exerts these effects is yet to be elucidated. Given the role of cholesterol in the RBC membrane, it is plausible that cholesterol regulates cell survival. However, the function of the CSP might not be limited to cell death or stress mechanisms because previously published work has indicated a regulatory

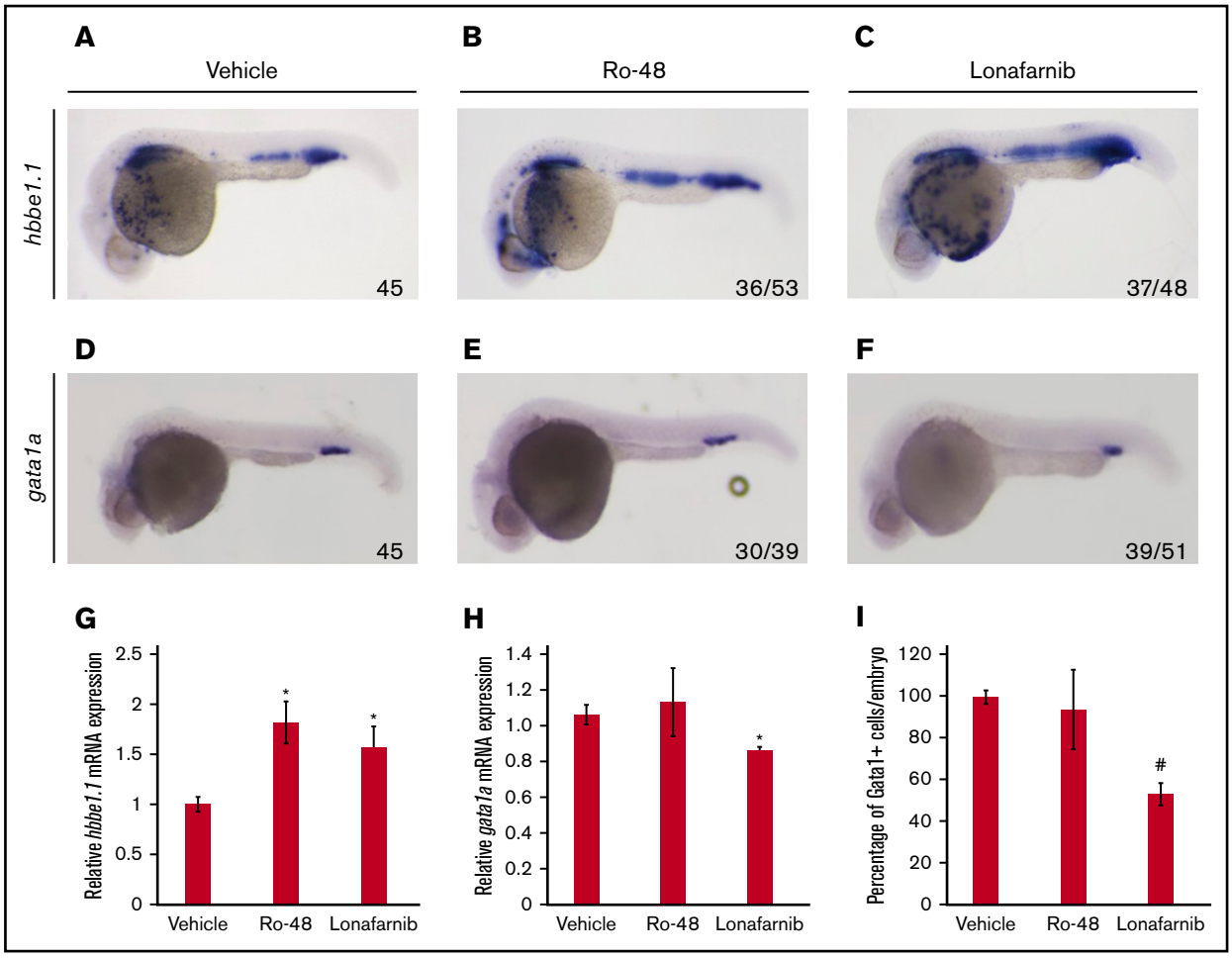

Figure 5. Isoprenoids regulate RBC development in a *gata1a*-dependent manner. (A-F) Embryos were treated at sphere stage with Ro-48 to inhibit cholesterol, lonafarnib to inhibit isoprenoids, or vehicle control (DMSO). At 26 hpf, whole mount ISH was performed to detect *hbbe1.1* (n = 45 DMSO, n = 53 Ro-48 [$P = .0001$], and n = 48 lonafarnib [$P = .0001$]) (A-C) or *gata1a* (D-F) expression (n = 45 DMSO, n = 39 Ro-48 [NS], and n = 51 lonafarnib; [$P = .0001$]). Total embryos were obtained with a minimum 3 biological replicates. Images were taken with a 10× optical lens at 6.3× objective zoom. *P* value designates statistical significance relative to vehicle control according to a Fisher's exact test. Total RNA was isolated from embryos treated with vehicle control (DMSO), Ro-48, or lonafarnib; qPCR was performed to detect the expression of *hbbe1.1* (G) or *gata1a* (H). All samples were performed in technical triplicate and error bars represent the standard deviation of technical triplicates. *$P < .05$. (I) *Tg*(*gata1a*:dsRed) embryos were treated at sphere stage with Ro-48 to inhibit cholesterol, lonafarnib to inhibit isoprenoids, or vehicle control (DMSO). Fluorescence was visualized using a confocal microscope. The number of cells/Z-stack was quantified using ImageJ. #$P = 2.7125e-07$.

function for cholesterol and its derivatives at the level of cellular differentiation.[56-63] Future work that analyzes both primitive and definitive hematopoiesis at unique stages of differentiation in different model systems is likely to identify the exact cellular mechanisms underlying the phenotypic alteration we describe. The closely related zebrafish mutant of *hmgcrb* will be of great utility because we hypothesize that mutation of *hmgcrb*[37] will produce overlapping phenotypes with the Vu57 allele.

The GATA family of transcription factors are essential mediators of erythropoiesis. Specifically, the expression of *GATA1* signals the commitment of a common myeloid progenitor toward an erythroid fate. Numerous studies have confirmed that the expression of *GATA1* is at the center of at least 2 axis-governing cell fate decisions. The expression of *GATA1* represses the expression of *GATA2*, a second member of the family whose expression promotes a progenitor cell fate.[15,64] GATA1 expression also antagonizes the expression of *SPI-1*, which promotes myeloid differentiation.[65,66] Here we demonstrate for the first time that the expression of *gata1a*, the zebrafish ortholog of *GATA1*, is linked to the CSP. Moreover, we establish that expression of *gata1a* is isoprenoid dependent. These data are supported by previously published studies by Quintana et al, which demonstrate that defects in cholesterol synthesis disrupt RBC differentiation without disrupting early *gata1a* expression.[24] Despite reduced expression of *gata1a* in *hmgcs1* mutants, differentiating RBCs maintain their ability to initiate and maintain *globin* and *alas2* expression. The inhibition of the CSP did not cause the excessive accumulation of mature RBCs to other bodily regions except for in the presence of atorvastatin treatment, where cerebral hemorrhages are observed. This phenotype is not consistently observed with the Vu57 allele or larvae treated with lonafarnib or Ro 48 8071, but has been reported in *hmgcrb* mutants.[37] Despite the presence of cerebral hemorrhages in atorvastatin-treated embryos, we still

observe a statistically significant decrease in total hemoglobin content in these larvae. Thus, suggesting that inhibition of the CSP reduces total hemoglobin content, which is consistent with an accumulation of *globin* and *alas2* RNA. These results are further supported by in vitro studies of *GATA1* deletion where *GATA1* negative cells undergo developmental arrest, but maintain expression of GATA target genes, including globin.[67]

Our data establish that isoprenoid synthesis is essential for appropriate *gata1a* expression. These effects are likely to be indirect because isoprenoids are a large class of molecules with diverse functions. Retinoids are an isoprenoid derivative[68] and retinoic acid is 1 potential regulator of blood cell differentiation because previous studies have established that retinoic acid signaling increases the number of HSCs[30,31,33] and mediates the formation of HSCs from the mesoderm.[69] However, these mechanisms are likely to be complex and stage specific because retinoic acid has been shown to decrease the expression of *gata1* in zebrafish.[70] Thus, retinoic acid is only 1 potential mediator of erythropoiesis.

Here we demonstrate that cholesterol and isoprenoids, 2 products of the CSP modulate RBC differentiation in vivo. The cholesterol independent mechanisms disrupt *gata1a* expression and the number of Gata1a^{+} cells produced. This is notable as GATA1 regulates at least 2 axis-regulating lineage fate decisions, but it is not clear if there are hematopoietic defects before onset of *gata1a* expression. The presence of cerebral hemorrhages in atorvastatin-treated embryos may shed some light on this question because HSCs and endothelial cell progenitors both arise from a common bipotent progenitor during primitive hematopoiesis.[71,72] Thus, defects in both lineages could indicate early defects in the formation or differentiation of cells from mesoderm. Future studies that define the mechanisms by which cholesterol and isoprenoids regulate all stages of differentiation, including early HSCs and myeloid cells, are warranted.

Our study focuses on the regulation of *GATA1* expression, primarily in the context of isoprenoids. Given the role of isoprenoids in development and signaling, it is likely that they are positive upstream regulators of *gata1a*. Therefore, future work in this area may identify novel therapeutic targets for various disorders. For example, mutation of mevalonate kinase causes mevalonate kinase deficiency.[73,74] Mevalonate kinase is central to the CSP and converts mevalonate to 5′phosphomevalonate, which is the substrate for future enzymatic reactions that culminate with the creation of cholesterol and isoprenoids and therefore mutations in this kinase disrupt the synthesis of both cholesterol and isoprenoids. Patients with mevalonate kinase deficiency exhibit hematological deficiencies and extramedullary hematopoiesis,[75] but the mechanisms underlying these phenotypes are not fully characterized. However, mutations in mevalonate kinase are likely to be recapitulated in zebrafish with mutations in *hmgcs1* or *hmgcrb*. Therefore, our system has the potential to understand the mechanisms governing *GATA1* expression, a central transcriptional regulator of primitive hematopoiesis.

Acknowledgments

The *hmgcs1*^{Vu57} allele was kindly provided by Bruce Appel from the University of Colorado Anschutz Medical Campus. The *Tg*(*gata1a*:dsRed) fish were provided by Leonard Zon from Harvard Medical School.

These studies were supported by grants from the National Institutes of Health, National Institute on Minority Health and Health Disparities (2G12MD007592) to the University of Texas El Paso; National Institutes of Health, National Institutes of General Medical Sciences (RL5GM118969, TL4GM118971, R25GM069621-11, and UL1GM118970) to the University of Texas El Paso; and National Institutes of Health, National Institute of Neurological Disorders and Stroke (1K01NS099153-01A1) (A.M.Q.).

Authorship

Contribution: J.A.H. and A.M.Q. synthesized the hypothesis, performed in situ hybridization, genotyping, data analysis, statistical analysis, cell counts, wrote the manuscript, and performed study design; J.A.H. and V.L.C. performed quantitative polymerase chain reaction; A.M.Q. and V.L.C. performed morpholino injections and hemoglobin quantification in drug treatment assays; V.L.C. performed *o*-dianisidine staining, imaged, and contributed to data analysis; N.R.-N. and J.A.H. performed genotyping and imaging; and J.A.H. and L.P.M. performed hemoglobin quantification in fish harboring the Vu57 allele.

Conflict-of-interest disclosure: The authors declare no competing financial interests.

Correspondence: Anita M. Quintana, Department of Biological Sciences, University of Texas El Paso, 500 W University Ave, Biosciences Building, Room 5.150, El Paso, TX 79968; e-mail: aquintana8@utep.edu.

References

1. Weinstein BM, Schier AF, Abdelilah S, et al. Hematopoietic mutations in the zebrafish. *Development*. 1996;123:303-309.
2. Dzierzak E, Philipsen S. Erythropoiesis: development and differentiation. *Cold Spring Harb Perspect Med*. 2013;3(4):a011601.
3. Vlachos A, Blanc L, Lipton JM. Diamond Blackfan anemia: a model for the translational approach to understanding human disease. *Expert Rev Hematol*. 2014;7(3):359-372.
4. Frey H, Moreth K, Hsieh LT-H, et al. A novel biological function of soluble biglycan: Induction of erythropoietin production and polycythemia. *Glycoconj J*. 2017;34(3):393-404.
5. Sandes AF, Gonçalves MV, Chauffaille ML. Frequency of polycythemia in individuals with normal complete blood cell counts according to the new 2016 WHO classification of myeloid neoplasms. *Int J Lab Hematol*. 2017;39(5):528-531.
6. Spivak JL. Polycythemia vera. *Curr Treat Options Oncol*. 2018;19(2):12.
7. Mettananda S, Fisher CA, Hay D, et al. Editing an α-globin enhancer in primary human hematopoietic stem cells as a treatment for β-thalassemia. *Nat Commun*. 2017;8(1):424.

8. Perkins A, Xu X, Higgs DR, et al; KLF1 Consensus Workgroup. Krüppeling erythropoiesis: an unexpected broad spectrum of human red blood cell disorders due to KLF1 variants. *Blood*. 2016;127(15):1856-1862.

9. Olivieri NF. Fetal erythropoiesis and the diagnosis and treatment of hemoglobin disorders in the fetus and child. *Semin Perinatol*. 1997; 21(1):63-69.

10. Fahnenstich H, Dame C. Erythropoietin concentrations and erythropoiesis in newborns suffering from renal agenesis and congenital kidney diseases. *Eur J Pediatr*. 1996;155(3):185-188.

11. Wakabayashi A, Ulirsch JC, Ludwig LS, et al. Insight into GATA1 transcriptional activity through interrogation of cis elements disrupted in human erythroid disorders. *Proc Natl Acad Sci USA*. 2016;113(16):4434-4439.

12. Ling T, Crispino JD, Zingariello M, Martelli F, Migliaccio AR. GATA1 insufficiencies in primary myelofibrosis and other hematopoietic disorders: consequences for therapy. *Expert Rev Hematol*. 2018;11(3):169-184.

13. Sonoda M, Ishimura M, Ichimiya Y, et al. Atypical erythroblastosis in a patient with Diamond–Blackfan anemia who developed del(20q) myelodysplasia. *Int J Hematol*. 2018;108(2):1-4.

14. O'Brien KA, Farrar JE, Vlachos A, et al. Molecular convergence in ex vivo models of Diamond-Blackfan anemia. *Blood*. 2017;129(23):3111-3120.

15. Orkin SH. GATA-binding transcription factors in hematopoietic cells. *Blood*. 1992;80(3):575-581.

16. Hasegawa A, Kaneko H, Ishihara D, et al. GATA1 binding kinetics on conformation-specific binding sites elicit differential transcriptional regulation. *Mol Cell Biol*. 2016;36(16):2151-2167.

17. Rifkind JM, Nagababu E. Hemoglobin redox reactions and red blood cell aging. *Antioxid Redox Signal*. 2013;18(17):2274-2283.

18. Chen Q, Fabry ME, Rybicki AC, et al. A transgenic mouse model expressing exclusively human hemoglobin E: indications of a mild oxidative stress. *Blood Cells Mol Dis*. 2012;48(2):91-101.

19. Ziobro A, Duchnowicz P, Mulik A, Koter-Michalak M, Broncel M. Oxidative damages in erythrocytes of patients with metabolic syndrome. *Mol Cell Biochem*. 2013;378(1-2):267-273.

20. Hernández-Muñoz R, Olguín-Martínez M, Aguilar-Delfín I, et al. Oxidant status and lipid composition of erythrocyte membranes in patients with type 2 diabetes, chronic liver damage, and a combination of both pathologies. *Oxid Med Cel. Longev*. 2013;2013:657387.

21. Sharif NF, Korade Z, Porter NA, Harrison FE. Oxidative stress, serotonergic changes and decreased ultrasonic vocalizations in a mouse model of Smith-Lemli-Opitz syndrome. *Genes Brain Behav*. 2017;16(6):619-626.

22. Ghezzo A, Visconti P, Abruzzo PM, et al. Oxidative stress and erythrocyte membrane alterations in children with autism: correlation with clinical features. *PLoS One*. 2013;8(6):e66418.

23. Mejia-Pous C, Damiola F, Gandrillon O. Cholesterol synthesis-related enzyme oxidosqualene cyclase is required to maintain self-renewal in primary erythroid progenitors. *Cell Prolif*. 2011;44(5):441-452.

24. Quintana AM, Picchione F, Klein Geltink RI, Taylor MR, Grosveld GC. Zebrafish ETV7 regulates red blood cell development through the cholesterol synthesis pathway. *Dis Model Mech*. 2014;7(2):265-270.

25. Rodriguez JB, Falcone BN, Szajnman SH. Approaches for designing new potent inhibitors of farnesyl pyrophosphate synthase. *Expert Opin Drug Discov*. 2016;11(3):307-320.

26. McTaggart SJ. Isoprenylated proteins. *Cell Mol Life Sci*. 2006;63(3):255-267.

27. Murthy S, Tong H, Hohl RJ. Regulation of fatty acid synthesis by farnesyl pyrophosphate. *J Biol Chem*. 2005;280(51):41793-41804.

28. Westerterp M, Gourion-Arsiquaud S, Murphy AJ, et al. Regulation of hematopoietic stem and progenitor cell mobilization by cholesterol efflux pathways. *Cell Stem Cell*. 2012;11(2):195-206.

29. Tall AR, Yvan-Charvet L, Westerterp M, Murphy AJ. Cholesterol efflux: a novel regulator of myelopoiesis and atherogenesis. *Arterioscler Thromb Vasc Biol*. 2012;32(11):2547-2552.

30. Cabezas-Wallscheid N, Buettner F, Sommerkamp P, et al. Vitamin A-Retinoic Acid Signaling Regulates Hematopoietic Stem Cell Dormancy. *Cell*. 2017; 169(5):807-823.

31. Chanda B, Ditadi A, Iscove NN, Keller G. Retinoic acid signaling is essential for embryonic hematopoietic stem cell development. *Cell*. 2013; 155(1):215-227.

32. Pillay LM, Mackowetzky KJ, Widen SA, Waskiewicz AJ. Somite-derived retinoic acid regulates zebrafish hematopoietic stem cell formation. *PLoS One*. 2016;11(11):e0166040.

33. Rundberg Nilsson A, Pronk CJ. Retinoic acid puts hematopoietic stem cells back to sleep. *Cell Stem Cell*. 2017;21(1):9-11.

34. Traver D, Paw BH, Poss KD, Penberthy WT, Lin S, Zon LI. Transplantation and in vivo imaging of multilineage engraftment in zebrafish bloodless mutants. *Nat Immunol*. 2003;4(12):1238-1246.

35. Mathews ES, Mawdsley DJ, Walker M, Hines JH, Pozzoli M, Appel B. Mutation of 3-hydroxy-3-methylglutaryl CoA synthase I reveals requirements for isoprenoid and cholesterol synthesis in oligodendrocyte migration arrest, axon wrapping, and myelin gene expression. *J Neurosci*. 2014;34(9): 3402-3412.

36. Quintana AM, Hernandez JA, Gonzalez CG. Functional analysis of the zebrafish ortholog of HMGCS1 reveals independent functions for cholesterol and isoprenoids in craniofacial development. *PLoS One*. 2017;12(7):e0180856.

37. Eisa-Beygi S, Hatch G, Noble S, Ekker M, Moon TW. The 3-hydroxy-3-methylglutaryl-CoA reductase (HMGCR) pathway regulates developmental cerebral-vascular stability via prenylation-dependent signalling pathway. *Dev Biol*. 2013;373(2):258-266.

38. Mathews ES, Appel B. Cholesterol biosynthesis supports myelin gene expression and axon ensheathment through modulation of P13K/Akt/mTor signaling. *J Neurosci*. 2016;36(29):7628-7639.

39. Thoma R, Schulz-Gasch T, D'Arcy B, et al. Insight into steroid scaffold formation from the structure of human oxidosqualene cyclase. *Nature*. 2004; 432(7013):118-122.

40. Shenoy SD, Spencer TA, Mercer-Haines NA, et al. Induction of CYP3A by 2,3-oxidosqualene:lanosterol cyclase inhibitors is mediated by an endogenous squalene metabolite in primary cultured rat hepatocytes. *Mol Pharmacol*. 2004;65(5):1302-1312.

41. Taveras AG, Aki C, Chao J, et al. Exploring the role of bromine at C(10) of (+)-4-[2-[4-(8-chloro-3,10-dibromo- 6,11-dihydro-5H-benzo[5,6]cyclohepta[1,2-b]pyridin-11(R)-yl)-1-piperidinyl]-2- oxoethyl]-1-piperidinecarboxamide (Sch-66336): the discovery of indolocycloheptapyridine inhibitors of farnesyl protein transferase. *J Med Chem*. 2002;45(18):3854-3864.

42. Paffett-Lugassy NN, Zon LI. Analysis of hematopoietic development in the zebrafish. *Methods Mol Med*. 2005;105:171-198.

43. Thisse C, Thisse B. High-resolution in situ hybridization to whole-mount zebrafish embryos. *Nat Protoc*. 2008;3(1):59-69.

44. Willett CE, Cortes A, Zuasti A, Zapata AG. Early hematopoiesis and developing lymphoid organs in the zebrafish. *Dev Dyn*. 1999;214(4):323-336.

45. Ghneim HK, Alshebly MM. Biochemical markers of oxidative stress in saudi women with recurrent miscarriage. *J Korean Med Sci*. 2016;31(1):98-105.

46. Harigae H, Suwabe N, Weinstock PH, et al. Deficient heme and globin synthesis in embryonic stem cells lacking the erythroid-specific delta-aminolevulinate synthase gene. *Blood*. 1998;91(3):798-805.

47. Ogawa-Otomo A, Kurisaki A, Ito Y. Aminolevulinate synthase 2 mediates erythrocyte differentiation by regulating larval globin expression during Xenopus primary hematopoiesis. *Biochem Biophys Res Commun*. 2015;456(1):476-481.

48. Bresciani E, Confalonieri S, Cermenati S, et al. Zebrafish numb and numblike are involved in primitive erythrocyte differentiation. *PLoS One*. 2010; 5(12):e14296.

49. Rampon C, Bouzaffour M, Ostuni MA, et al. Translocator protein (18 kDa) is involved in primitive erythropoiesis in zebrafish. *FASEB J*. 2009; 23(12):4181-4192.

50. Sirtori CR. The pharmacology of statins. *Pharmacol Res*. 2014;88:3-11.

51. Aslan A, Borcek AO, Pamukcuoglu S, Baykaner MK. Intracranial undifferentiated malign neuroglial tumor in Smith-Lemli-Opitz syndrome: a theory of a possible predisposing factor for primary brain tumors via a case report. *Childs Nerv Syst*. 2017;33(1):171-177.

52. Ohashi K, Osuga J, Tozawa R, et al. Early embryonic lethality caused by targeted disruption of the 3-hydroxy-3-methylglutaryl-CoA reductase gene. *J Biol Chem*. 2003;278(44):42936-42941.

53. Porter FD, Herman GE. Malformation syndromes caused by disorders of cholesterol synthesis. *J Lipid Res*. 2011;52(1):6-34.

54. Quarfordt SH, Hilderman HL. Quantitation of the in vitro free cholesterol exchange of human red cells and lipoproteins. *J Lipid Res*. 1970;11(6):528-535.

55. Lange Y, Molinaro AL, Chauncey TR, Steck TL. On the mechanism of transfer of cholesterol between human erythrocytes and plasma. *J Biol Chem*. 1983;258(11):6920-6926.

56. Soroosh P, Wu J, Xue X, et al. Oxysterols are agonist ligands of RORγt and drive Th17 cell differentiation. *Proc Natl Acad Sci USA*. 2014; 111(33):12163-12168.

57. Hu X, Wang Y, Hao L-Y, et al. Sterol metabolism controls T(H)17 differentiation by generating endogenous RORγ agonists [published correction appears in *Nat Chem Biol*. 2015;11(9):741]. *Nat Chem Biol*. 2015;11(2):141-147.

58. Shan NL, Wahler J, Lee HJ, et al. Vitamin D compounds inhibit cancer stem-like cells and induce differentiation in triple negative breast cancer. *J Steroid Biochem Mol Biol*. 2017;173:122-129.

59. Cartocci V, Segatto M, Di Tunno I, Leone S, Pfrieger FW, Pallottini V. Modulation of the isoprenoid/cholesterol biosynthetic pathway during neuronal differentiation in vitro. *J Cell Biochem*. 2016;117(9):2036-2044.

60. Driver AM, Kratz LE, Kelley RI, Stottmann RW. Altered cholesterol biosynthesis causes precocious neurogenesis in the developing mouse forebrain. *Neurobiol Dis*. 2016;91:69-82.

61. Olivier E, Dutot M, Regazzetti A, et al. Lipid deregulation in UV irradiated skin cells: Role of 25-hydroxycholesterol in keratinocyte differentiation during photoaging. *J Steroid Biochem Mol Biol*. 2017;169:189-197.

62. Hlaing SM, Garcia LA, Contreras JR, Norris KC, Ferrini MG, Artaza JN. 1,25-Vitamin D3 promotes cardiac differentiation through modulation of the WNT signaling pathway. *J Mol Endocrinol*. 2014;53(3):303-317.

63. Cabral-Teixeira J, Martinez-Fernandez A, Cai W, Terzic A, Mercola M, Willems E. Cholesterol-derived glucocorticoids control early fate specification in embryonic stem cells. *Stem Cell Res (Amst)*. 2015;15(1):88-95.

64. Kaimakis P, de Pater E, Eich C, et al. Functional and molecular characterization of mouse Gata2-independent hematopoietic progenitors. *Blood*. 2016; 127(11):1426-1437.

65. Arinobu Y, Mizuno S, Chong Y, et al. Reciprocal activation of GATA-1 and PU.1 marks initial specification of hematopoietic stem cells into myeloerythroid and myelolymphoid lineages. *Cell Stem Cell*. 2007;1(4):416-427.

66. Zhang P, Behre G, Pan J, et al. Negative cross-talk between hematopoietic regulators: GATA proteins repress PU.1. *Proc Natl Acad Sci USA*. 1999; 96(15):8705-8710.

67. Weiss MJ, Keller G, Orkin SH. Novel insights into erythroid development revealed through in vitro differentiation of GATA-1 embryonic stem cells. *Genes Dev*. 1994;8(10):1184-1197.

68. Kedishvili NY. Retinoic acid synthesis and degradation. *Subcell Biochem*. 2016;81:127-161.

69. Cañete A, Cano E, Muñoz-Chápuli R, Carmona R. Role of vitamin a/retinoic acid in regulation of embryonic and adult hematopoiesis. *Nutrients*. 2017; 9(2):E159.

70. de Jong JLO, Davidson AJ, Wang Y, et al. Interaction of retinoic acid and scl controls primitive blood development. *Blood*. 2010;116(2):201-209.

71. Muñoz-Chápuli R, Pérez-Pomares JM, Macías D, García-Garrido L, Carmona R, González M. Differentiation of hemangioblasts from embryonic mesothelial cells? A model on the origin of the vertebrate cardiovascular system. *Differentiation*. 1999;64(3):133-141.

72. Xiong J-W. Molecular and developmental biology of the hemangioblast. *Dev Dyn*. 2008;237(5):1218-1231.

73. Favier LA, Schulert GS. Mevalonate kinase deficiency: current perspectives. *Appl Clin Genet*. 2016;9:101-110.

74. Tricarico PM, Marcuzzi A, Piscianz E, Monasta L, Crovella S, Kleiner G. Mevalonate kinase deficiency and neuroinflammation: balance between apoptosis and pyroptosis. *Int J Mol Sci*. 2013;14(12):23274-23288.

75. Hinson DD, Rogers ZR, Hoffmann GF, et al. Hematological abnormalities and cholestatic liver disease in two patients with mevalonate kinase deficiency. *Am J Med Genet*. 1998;78(5):408-412.